Immunobiology 224 (2019) 792–803

Contents lists available at ScienceDirect

Immunobiology

journal homepage: www.elsevier.com/locate/imbio

# RAGE and CCR7 mediate the transmigration of Zika-infected monocytes through the blood-brain barrier*

Gabriel Costa de Carvalho[a,b], Marie-Yolande Borget[a], Stéphane Bernier[a], Daniel Garneau[a], Alberto José da Silva Duarte[b], Nancy Dumais[a,*]

[a] Département de Biologie, Faculté des Sciences, Université de Sherbrooke, 2500 boul de l'Université, Sherbrooke, QC, Canada
[b] Laboratory of Dermatology and Immunodeficiencies, LIM-56, Department of Dermatology, Medical School, Institute of Tropical Medicine, University of São Paulo, São Paulo, Brazil

ARTICLE INFO

*Keywords:*
Zika virus
Monocytes
Blood-brain barrier
RAGE
CCR7
HMGB1

ABSTRACT

Details of the "Trojan Horse" mechanism by which Zika virus (ZIKV) crosses the blood-brain barrier (BBB) remain unclear. However, the migration of ZIKV-infected monocytes to the brain is thought to be dependent on both pattern-recognition and chemokine receptors. In this study, we investigated whether the migration of ZIKV-infected MonoMac-1 (MM-1) cells through the BBB is dependent on chemokine receptor 7 (CCR7) and receptor for advanced glycation end (RAGE); we also determined whether high mobility group box protein 1 (HMGB1) could facilitate the permeabilization of endothelial cells. We demonstrated that ZIKV infects MM-1 cells, leading to milieu accumulation of HMGB1. Our results suggest that HMGB1 is involved in the dysregulation of primary human brain microvascular endothelial cell junction markers. Our results also indicate that the migration of ZIKV-infected monocytes is dependent on chemokine ligand 19 (CCL19), the natural ligand of CCR7, in conditions recapitulating inflammation. RAGE-dependent migration of ZIKV-infected cells declined during transmigration assays in the presence of RAGE receptor antagonist FPS-ZM1. Understanding the molecular role of monocyte trafficking during ZIKV infections could facilitate the development of new therapeutic strategies to prevent the deleterious consequences of ZIKV neuroinfection.

## 1. Introduction

Several viruses of the *Flavivirus* genus are capable of invading the central nervous system (CNS) and are regarded as neurotropic viruses (Neal, 2014) that cause inflammation (Ludlow et al., 2016). Among these, the Zika virus (ZIKV), which is transmitted by *Aedes* spp. mosquitoes (Dick et al., 1952), is associated with microcephaly and congenital infection (Schuler-Faccini et al., 2016). Monocytes are closely associated with ZIKV transmission and pathogenesis (Foo et al., 2017; Michlmayr et al., 2017), and the percentage of infected $CD14^+$ $CD16^+$ monocytes increases during ZIKV infection (Foo et al., 2017; Michlmayr et al., 2017; Kam et al., 2017). After replicating in cells and regional lymph nodes located near sites where infected mosquitoes have bitten a host, ZIKV can spread to other organs and tissues, including the CNS, skeletal muscle, myocardium, and placenta (Dick et al., 1952). To infect the fetal brain, the virus must cross both the placental barrier and the fetal blood-brain barrier (BBB) (Delorme-Axford et al., 2014; Tabata et al., 2016). One mechanism for crossing the BBB involves direct infection of endothelial cells and subsequent crossing of the membrane by virus particles (Weksler et al., 2013; Liu et al., 2016; Papa et al., 2017). In addition, the virus can be transported through the CNS by infected leukocytes via a neuroinvasion mechanism known as "Trojan Horse" (Miner and Diamond, 2016).

The nuclear high mobility group box protein 1 (HMGB1), a danger-associated molecular pattern (DAMP) molecule, is secreted by activated macrophages, mature dendritic cells (DCs), natural killer cells, keratinocytes, and other cells in response to cellular damage, infections, and inflammatory stress (West et al., 2004; Zeh and Lotze, 2005; Park et al., 2006; Stros, 2010). Although the exact role of HMGB1 during viral infections is not clear, infections with influenza, human immunodeficiency virus type-1 (HIV), and herpes simplex type-2 (HSV-2) have been associated with the release of extracellular HMGB1 (Nowak et al., 2007; Ito et al., 2011; Borde et al., 2011). During *Flavivirus* infections, the passive release of HMGB1 into the extracellular environment has been observed. For West Nile virus (WNV) infections, an accumulation of HMGB1 has been shown to cause inflammation that not

* Claus Kerkhoff – in memoriam – Department of Biomedical Sciences, School of Human Sciences, University of Osnabrueck, Germany.

* Corresponding author at: Département de Biologie, Faculté des Sciences, Université de Sherbrooke, 2500 boul de l'Université, Sherbrooke, QC, J1K 2R1, Canada.
*E-mail address:* nancy.dumais@usherbrooke.ca (N. Dumais).

https://doi.org/10.1016/j.imbio.2019.08.007
Received 3 June 2019; Received in revised form 12 July 2019; Accepted 22 August 2019
Available online 25 August 2019
0171-2985/ © 2019 Elsevier GmbH. All rights reserved.

only contributes to a pathogenic state but also to encephalitis (Chu and Ng, 2003). Similarly, high circulating levels of HMGB1 have been found within the first few days after onset of symptoms in Dengue virus (DENV) infection (Allonso et al., 2012). Moreover, the release of HMGB1 during DENV infection of peripheral blood mononuclear cells (PBMCs) induces vascular permeability into umbilical cord vein endothelial cells (Ong et al., 2012).

Extracellular HMGB1 binds to pattern-recognition receptors, including Toll-like receptors (TLRs) and the receptor for advanced glycation end products (RAGE), and induces inflammatory responses (Bonaldi et al., 2003; Park et al., 2004; Dumitriu et al., 2005; Lotze and Tracey, 2005; Yu et al., 2006; Bamboat et al., 2010; Vande Walle et al., 2011). HMGB1 promotes monocyte recruitment by activating the RAGE/nuclear factor (NF)-κB signaling pathway (Vogel et al., 2016). Further, RAGE is involved in cell migration, and DAMP molecules such as amyloid beta peptide can bind to RAGE and induce monocyte migration across human brain microvascular endothelial cell (HBMEC) layers (Yan et al., 1996). RAGE has been implicated in the pathogenesis of various neurodegenerative diseases, such as amyotrophic lateral sclerosis, Alzheimer, Parkinson, and Huntington disease (Schmidt et al., 2001; Brenn et al., 2011; Anzilotti et al., 2012; Teismann, 2012). In adult tissues, RAGE is expressed in endothelial cells, monocytes, microglia, and neurons. RAGE expression is upregulated upon interaction with HMGB1 protein, which induces monocytes to produce TNF-α, IL-1β, IL-6, and IL-8 (Yan et al., 1996; Andersson et al., 2000).

The chemokine receptor CCR7 plays an essential role in the migratory behavior of monocytes. CCR7 is expressed in DCs (Saeki et al., 1999), T and B cells (Warnock et al., 2000), and monocytes (Coté et al., 2009). Its natural ligands, CCL19 and CCL21, are essential for cellular migration: CCL19 is known to be constitutively expressed in the CNS (McGavern and Kang, 2011) and upregulated during inflammation, infection, and cancer (Columba-Cabezas et al., 2003; Krumbholz et al., 2007). Using an *in vitro* human BBB model with HBMECs and primary human neuronal astrocytes (NHAs), our group demonstrated that TLR4 activation increased the CCR7-dependent transmigration of monocytes through the BBB (Paradis et al., 2016a,b).

To understand whether ZIKV-infected monocytes act as a Trojan Horse to transport the virus through the BBB, we studied the effects of HMGB1, RAGE, and CCR7 on the transmigration of infected monocytes through the BBB. We demonstrate that ZIKV infects MonoMac-1 (MM-1) cells that lead to the accumulation of HMGB1 in the milieu. Reverse transcription-quantitative polymerase chain reaction and immunofluorescence analyses were performed to assess the expression of junction markers such as zonula occludens-1 (ZO-1), occludin, and vascular endothelial (VE)-cadherin. Our results suggest that the presence of HMGB1 after ZIKV infection of monocytes might be involved in the endothelial activation of RAGE, resulting in dysregulation of HBMEC tight junctions. Our results also indicate that the migration of ZIKV-infected monocytes is dependent on CCL19, the natural ligand of CCR7, in conditions mimicking inflammation. The RAGE-dependent migration of ZIKV-infected cells was shown to decrease when the RAGE receptor antagonist, FPS-ZM1, was added prior to the transmigration assays. Understanding how monocytes migrate during *Flavivirus* infections could facilitate the development of new therapeutic strategies to prevent the deleterious consequences of such neuroinfections.

## 2. Materials and methods

### 2.1. Reagents

Lipopolysaccharide (LPS) from *Escherichia coli* 026:B6 was purchased from Sigma-Aldrich (Saint Louis, MO, USA). The chemokines CCL19 and CCL2 were purchased from R&D Systems (Minneapolis, MN, USA). ZIKV VR1838 was purchased from the American Type Culture Collection (ATCC) (Manassas, VA, USA).

### 2.2. Cell culture

Acute peripheral monoblastic leukemia-derived MM-1 cells (ACC252) (German Collection of Microorganisms and Cell Cultures, Braunschweig, Germany) were cultured in RPMI 1640 medium (Sigma-Aldrich) supplemented with 10% heat-inactivated fetal bovine serum (FBS), non-essential amino acids (NEAAs), 1 mM sodium pyruvate, 100 IU penicillin G, and 100 µg/mL streptomycin (all supplements were obtained from Wisent, St-Bruno, QC, Canada). The *in vitro* BBB model uses primary cultures of both HBMECs (ACBRI-376) and NHAs (ACBRI-371), both obtained from the Applied Cell Biology Research Institute (ACBRI) (Kirkland, WA, USA). HBMECs were cultured in CS-C complete serum-free medium (ABCRI, CSF-4Z0-500), and NHAs were cultured using a Complete Classic Medium Kit with Serum and CultureBoost (ABCRI, C4Z0-500). Antibiotic (BAC-OFF; ABCRI, 4Z0-643) was added to both media. Both primary cell lines were also cultured with attachment factors (ABCRI, 4Z0-210) and the Passage Reagent Group (ABCRI, 4Z0-800). Vero cells, an African monkey kidney cell line (ATCC CCL-81) were cultured and maintained in Eagle's minimum essential medium (Sigma-Aldrich) supplemented with 2% heat-inactivated FBS, NEAAs, 100 IU penicillin G, and 100 µg/mL streptomycin (Wisent).

### 2.3. Tissue culture infectious dose 50 (TCID50)

Vero cells were distributed in a 24-well plate and incubated at 37 °C until reaching a confluent monolayer of in each well. A suspension of ZIKV was diluted serially 10-fold, and an aliquot of each dilution was added to the plate (wells without virus served as a control). The plates were incubated at 37 °C for 48 h and observed for 7 days, at which time the number of positive and negative wells was recorded. TCID50/mL refer to the number of virus particles per milliliter capable of producing cytopathic effects in 50% of inoculated cells. The results were calculated according to the Reed & Muench method (Reed and Muench, 1938).

### 2.4. Real-time PCR

Total RNA was extracted from MM-1 cells or HBMECs using a RNeasy Plus Mini kit (Qiagen, Valencia, CA, USA), and reverse transcription was performed using a Sensiscript Reverse Transcriptase kit (Qiagen). The primers utilized for real-time PCR assays were as follows: RAGE, 5′-GAGGAGGAGCGTGCAGAACT-3′ forward, 5′-CCTCAAGGCC CTCCAGTACTACT-3′ reverse; HMGB1, 5′-CTCAGAGAGGTGGAAGACC ATGT-3′ forward, 5′-GGGATGTAGGTT TTCATTTCTCTTTC-3′ reverse; CCR7, 5′-GTGGTGGCTCTCCTTGTCAT-3′ forward, 5′-TGTGGTGTTGTC TCCGATGT-3′ reverse; CCR2, 5′-TGACAGGCACAGATGAATGG-3′ forward, 5′-ATCATCTCCTGGCTGAATGC-3′ reverse; TNFα 5′-GGCAGTCA GATCATCTTCTC-3′ forward, 5′-CTGGTTATCTCTCAGCTCCA-3′ reverse; IL-10, 5′-TGGAGGACTTTAAGGGTTAC3′ forward, 5′-GATGTCT GGGTCTTGGTTCT-3′ reverse; IL-1β, 5′-GGGCCTCAAGGAAAAGAATC -3′ forward, 5′-TTCTGCTTGAGAGGTGCTGA-3′ reverse; GAPDH, 5′-GAAGGTGAAGGTCGGAGT-3′ forward, 5′-GAAGATGGTGATGGGAT TTC-3′ reverse; occludin, 5′-GCAAAGTGAATGACAAGCGG-3′ forward, 5′-CACAGGCGAAGTTAATGGAAG-3′ reverse; zonula occludens (ZO-1), 5′-TGCTGAGTCCTTTGGTGATG-3′ forward, 5′-AATTTGGATCTCCGGG AAGAC-3′ reverse; and β-actin, 5′- CTAACTTGCGCAGAAAACAAGAT-3′ forward, 5′- TTCCTGTAACAACGCATCTCATA-3′ reverse. GAPDH or β-actin mRNA levels in all samples were used to normalize the mRNA content. PCR was performed using a CFX Connect real-time PCR Detection System (Bio-Rad, Mississauga, ON, Canada) with specific primers and SYBR Green (Applied Biosystems, Carlsbad, CA, USA) fluorescence detection reagents. The cycling protocol consisted of 10 min at 95 °C, followed by 40 cycles of 15 s at 95 °C and 60 s at 60 °C. Preliminary experiments were performed to ensure the linearity of the PCR results. The fold-increase in the expression of specific target mRNAs compared to normal controls was calculated according to the

$2^{-(\Delta\Delta Ct)}$ method.

### 2.5. Quantification of viral load

Quantification of ZIKV load in Vero or MM-1 cells was performed according to the RT-PCR/TaqMan technique adapted from Bayer et al. (2016). First, viral RNA was extracted using a QIAamp Viral RNA kit (Qiagen) according to the manufacturer's instructions. TaqMan Fast Virus 1-Step master mix reagent (Thermo Scientific) was used for RT-PCR, which was carried out using a CFX Connect Real-Time PCR Detection System (Bio-Rad). The primers and probes used were as follows: ZIKV, forward 5′CCGCTGCCCAACACAAG3′, reverse 5′CCACTAACGTT CTTTTGCAGACAT3′ and FAM–AGCCTACCTTGACAAGCAGTCAGACA CTCAA-MGB. The number of viral copies in the samples was estimated based on a standard curve prepared with known inoculum dilutions.

### 2.6. Chemotaxis assay

Chemotaxis was assessed by monitoring the migration of cells through a polycarbonate filter with 5-µm pore size in 96-well Transwell chambers (Millipore, Nepean, ON, Canada). The lower chamber contained 30 ng/mL of chemokine CCL2 or 300 ng/mL of chemokine CCL19 or medium alone as a control (to assess spontaneous migration). The upper chamber was loaded with MM-1 cells that had been infected 8 h earlier with ZIKV VR1838 [multiplicity of infection (MOI) of 0.5], cells that had been activated 8 h earlier with 0.1 µg/mL LPS, cells that had been both infected with ZIKV and activated with LPS 8 h earlier, or cells that were left unstimulated. The chambers were incubated for 4 h at 37 °C. Cells (in a 150-µL aliquot) that migrated to the bottom chamber were counted using a BD Accuri C6 flow cytometer (BD Accuri cytometers, Belgium) by acquiring events for a fixed time of 60 s using Accuri-C6 Plus software, version 1.0.23.1 (BD Biosciences). Spontaneous migration was subtracted to calculate specific migration. The percentage of migrated cells was calculated as follows: the number of cells that migrated in response to medium only was subtracted from the number of cells that migrated in response to medium supplemented with CCL2 or CCL19, and this number was reported according to the total input of cells. The data were reported as fold-increase. Each experiment was performed in triplicate and repeated a minimum of three times. LPS-activated cells were used as the positive control, whereas medium alone was the negative control for spontaneous migration, as described by Paradis et al. (2016a).

### 2.7. Model of chemotaxis through the BBB

Experiments employing the BBB model were performed as previously described by Paradis et al. (2016b). Six days after the initiation of BBB formation, the transendothelial electrical resistance (TEER) was measured using an ohm meter (EVOM; World Precision Instruments, Sarasota, FL, USA). For HBMECs combined with NHAs, the highest TEER was 180 ± 10 $\Omega cm^2$), and the lowest TEER was 150 ± 30 $\Omega$ $cm^2$. To prevent the presence of astrocytes in the lower chamber of the wells that might not have fully adhered to the external side of the membrane, we transferred each insert into a new plate. For safety purposes and to avoid viral contamination of our equipment, we measured the TEER prior to the assays. On the other hand, unstimulated MM-1 cells or cells treated with *N*-benzyl-4-chloro-*N*-cyclohexylbenzamide (FPS-ZM1, a RAGE inhibitor) did not significantly alter the TEER values (data not shown). The lower chamber contained 300 ng/mL of the chemokine CCL19 or Complete Classic Medium with serum alone as a control (to assess spontaneous migration), and the upper chamber contained MM-1 cells either stimulated with LPS (0.1 µg/mL), cells infected with ZIKV (MOI 0.5), or cells infected and LPS-activated simultaneously or left unstimulated. For migration inhibition assays, FPS-ZM1 was added (directly to ZIKV-infected cells or in the upper chamber of HBMEC cultures) at a concentration of 1, 10, or 100 nM and incubated for 2 h prior to the transmigration assay in a 24-well plate, which was incubated for 4 h at 37 °C. After incubation, cells that migrated to the bottom chamber (in a 150-µL aliquot) were washed twice in PBS + 3% BSA and counted using a BD Accuri C6 flow cytometer by acquiring events for a fixed time of 60 s using Accuri-C6 Plus software. To ensure that the barrier was sufficiently tight to allow only minimal cell migration, the TEER of all inserts was measured prior to all assays; each experiment was performed in triplicate and repeated at least three times.

### 2.8. Analysis of supernatant HMGB1 using an enzyme immunoassay

MM-1 cells were infected with ZIKV, activated with LPS (0.1 µg/mL), or infected and activated at the same time. After 2, 8, or 24 h, the cell supernatants were collected. HMGB1 protein in the supernatant of MM-1 cells was determined using an enzyme-linked immunosorbent assay (ELISA), according to the manufacturer's instructions (Chondrex, Redmond, WA, USA).

### 2.9. Assessment of apoptosis using annexin V and propidium iodide staining

Apoptosis of ZIKV-infected MM-1 cells was analyzed using an FITC Annexin V Apoptosis Detection Kit I (BD Biosciences, USA), according to the manufacturer's protocol. An initial ZIKV dilution of $10^{-2}$ from the stock were used for the assays with cells at a density of $1 \times 10^6$, and the cells were cultured for 24 h. Cells treated with normal culture medium or cells in which apoptosis was induced with DMSO were used as controls. The cells were analyzed by flow cytometry (BD Accure C6).

### 2.10. Immunofluorescence analysis of cells

HBMECs ($2 \times 10^5$/mL) were seeded into glass-well cell culture chambers (Sarstedt, Nümbrecht, Germany) and cultured until reaching 90% confluence. After 4 h of co-culture with MM-1 cells, the cells were stained by immunofluorescence. Briefly, cells were fixed using 4% paraformaldehyde (Sigma-Aldrich) in PBS for 10 min at room temperature. Permeabilization was performed using 0.1% Triton X-100 in PBS. After permeabilization, the cells were blocked with 5% FBS (Sigma-Aldrich), and the cell monolayer was incubated overnight with primary antibody against VE-cadherin (AF938) (R&D Systems, AF938) or RAGE (ab54741) (Abcam, Inc., Cambridge, UK). After washing, the corresponding secondary antibody NorthernLights™ 557–conjugated anti-goat IgG (NL001) or NorthernLights™ anti-mouse IgG-NL493 (R&D Systems) was added. For MM-1 staining, after ZIKV infection or treatment with 0.1 µg/mL LPS (TLR4), the cells were harvested, and anti-*Flavivirus* group antigen antibody (D1-4G2-4-15 [4G2]; R&D Systems), RAGE (ab54741) or HMGB1 (ab77302) (Abcam) were applied before the secondary antibody NorthernLights NL493 (R&D Systems). Nuclei were labeled with DAPI (1 µg/mL) (R&D Systems) in PBS. For controls, the primary antibody was omitted before the addition of the secondary antibody. Finally, the slides were mounted, and images were captured by confocal microscopy using an UPLAN SApo 40×/0.95 objective (Olympus FV3000; Olympus Corp., Tokyo, Japan) and Fluoview software (Olympus, Tokyo, Japan). The mean fluorescence intensity (MFI) of stained areas of the images was calculated using FIJI software (Madison, WI, USA) and Cellprofiler version 3.0.0 (Whitehead Institute and MIT, Cambridge, MA, USA).

### 2.11. Statistical analysis

All results were calculated as the mean ± SEM of independent experiments. Data were analyzed using GraphPad Prism6 by one-way ANOVA with Dunnett's correction for multiple comparisons. Differences were considered significant at the following $P$ values: * < 0.05, ** < 0.01, and *** < 0.001.

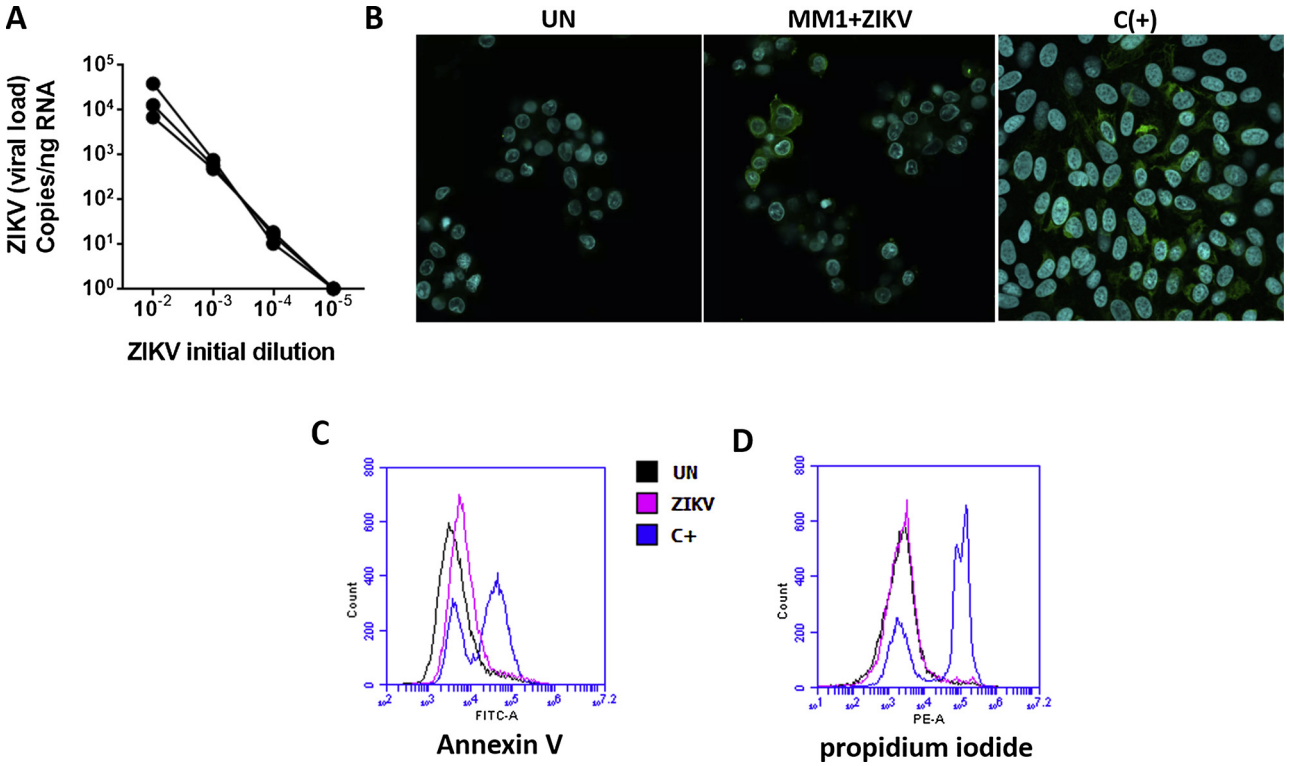


**Fig. 1.** ZIKV infection and the stimulation of apoptosis. MM-1 cells were infected with ZIKV for 24 h (MOI of 0.5). To detect ZIKV, RNA was extracted from the cells, and the viral load was determined by real-time PCR. An initial dilution of $10^{-2}$ from the stock was used for the assays (A). To identify ZIKV inside the cells, primary antibodies against anti-glycoprotein E (*Flavivirus*) and secondary antibody conjugated with Alexa Fluor-488 (green) were used. DAPI (blue) was utilized for the visualization of the cell nucleus (40×). Unstimulated cells were used as the negative control, and Vero cells previously infected with ZIKV were used as the positive control. (B). An annexin V/propidium iodide assay was performed to determine the viability of the cells (C, D). At least three independent experiments were performed. (For interpretation of the references to colour in this figure legend, the reader is referred to the web version of this article.)

## 3. Results

### 3.1. ZIKV infection of MM-1 cells

ZIKV (VIR1838) was produced in Vero cells (ATCC CCL-81) and quantified by the RT-PCR/TaqMan technique. We then determined whether ZIKV was capable of infecting MM-1 cells, a human monocyte line used to study monocyte function *in vitro* (Steube et al., 1997). Infections were established and titrated to determine the intracellular viral load after 24 h (Fig. 1A). At an MOI of 0.5 and at 24-h post infection, viral E protein was detected in the cytoplasm, clearly demonstrating viral infection of MM-1 cells (Fig. 1B). Unstimulated cells were used as a negative control; for the positive control, we used Vero cells (ATCC CCL-81) previously infected with ZIKV (VIR1838) (Fig. 1B). An annexin V/propidium iodide assay was performed to determine whether viral genetic material or viral E protein affected apoptosis during the early phase of infection. Experiments revealed no significant changes in apoptosis at 24 h after infection (Fig. 1C, D). These results demonstrate for the first time the capacity of MM-1 cells to be infected by ZIKV without the induction of apoptosis.

### 3.2. ZIKV infection induces HMGB1 release from MM-1 cells

LPS is recognized as an inducer of neuroinflammation and neurotoxicity, and is used to study neurological disorders (Abreu et al., 2018; Olajide et al., 2013; Gao et al., 2002; Hu et al., 2012; Kempuraj et al., 2017). Since neuroviruses are associated with inflammation, we used LPS in combination with ZIKV infection to study the transmigration of MM-1 through the BBB. First, we established whether HMGB1 production was modulated by ZIKV infection, as demonstrated for WNV and DENV (Chu and Ng, 2003; Allonso et al., 2012). We found that treatment of MM-1 cells with LPS, combined with ZIKV infection, resulted in the majority of HMGB1 being retained in the nucleus compared with other treatments (Fig. 2A, B). No differences were observed in the levels of HMGB1 in the cytoplasm after 8 h (Fig. 2A, C). Reduced HMGB1 mRNA expression was observed under all activation conditions compared with unstimulated MM-1 cells (Fig. 2D). Increased levels of HMGB1 were observed in the supernatant of LPS-treated and ZIKV-infected cells (Fig. 2E). We also found that MM-1 cells activated by LPS combined with ZIKV infection secreted more HMGB1 than did MM-1 cells treated with 0.1 μg/mL LPS after 8 h (Fig. 2E). After 24 h, LPS-treated MM-1 cells secreted increased levels of HMGB1 into the supernatant in comparison with all other conditions (Fig. 2F). These results demonstrate that extracellular levels of HMBG1 might be regulated by ZIKV infection.

### 3.3. ZIKV-infected MM-1 cells dysregulate tight junction markers upon contact with HBMECs

To determine whether ZIKV-infected MM-1 cells adversely affect HBMEC integrity, we evaluated various membrane junction markers. Eight hours after ZIKV infection (MOI of 0.5), MM-1 cells were co-cultivated for 4 h with a monolayer of HBMECs seeded in a culture chamber. We found that the MFI of the VE-cadherin protein declined in HBMECs that were in contact with ZIKV-infected MM-1 cells compared with monolayers of HBMECs co-cultivated with untreated LPS-treated MM-1 cells (Fig. 3A, B). Real-time PCR was used to evaluate the mRNA expression levels of junction marker in HBMECs co-cultured with MM-1 cells or HBMECs cultured alone. Expression of the VE-cadherin gene was downregulated in HBMECs that had previously been in contact with ZIKV-infected MM-1 cells compared with HBMECs that had been in contact with LPS-treated MM-1 cells (Fig. 3C). ZIKV infection or LPS

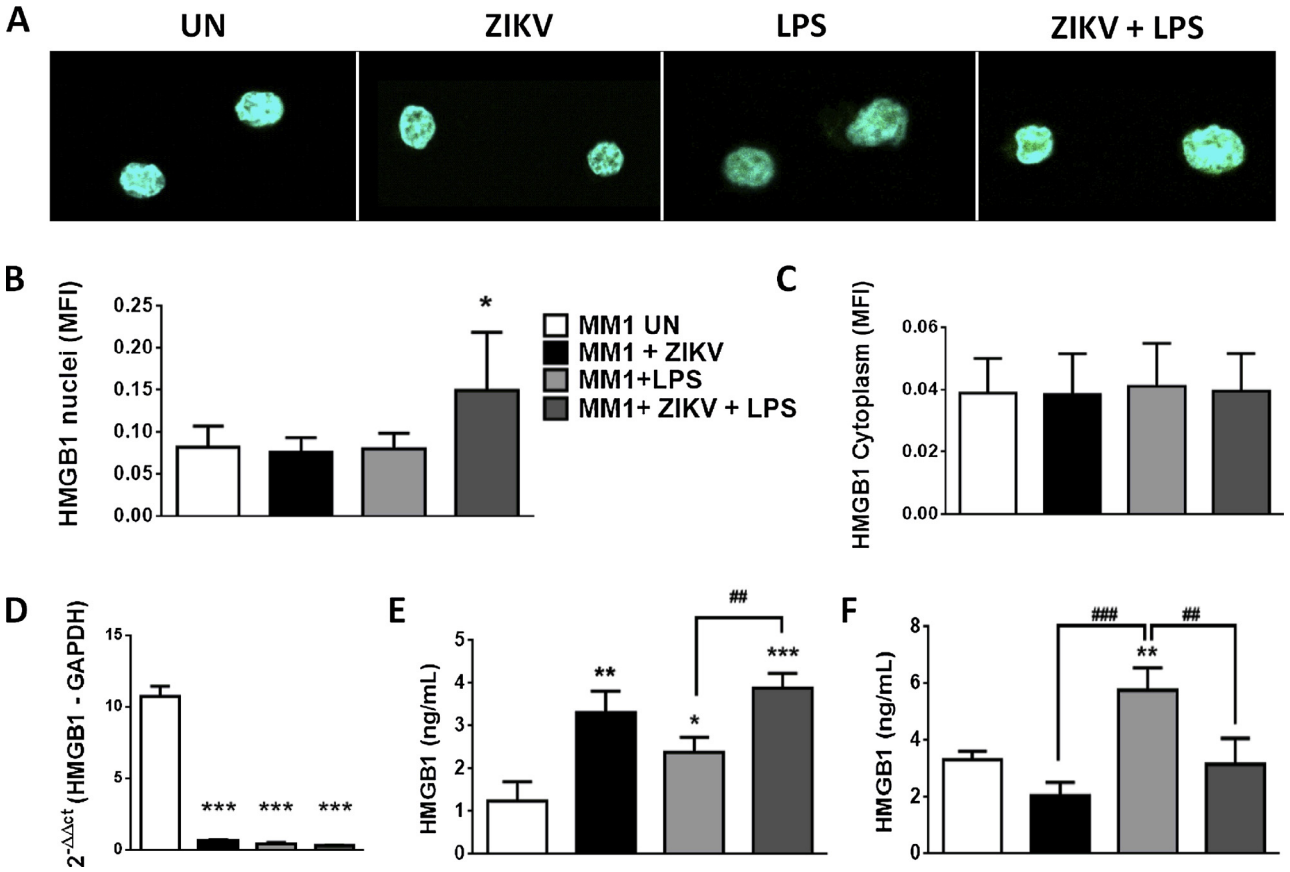


**Fig. 2.** MM-1 cells release HMGB1 during ZIKV infection without affecting levels in the cell nucleus/cytoplasm. MM-1 cells were infected with ZIKV (MOI of 0.5) and then treated or not with 0.1 μg/mL LPS for 8 h. Cells were then fixed with 4% paraformaldehyde. Primary antibodies against HMGB1 and NorthernLights NL493-conjugated secondary antibodies (green) were used. DAPI (blue) was utilized for the visualization of the cell nucleus (40×) (A). The MFI of the cells was measured in at least 10 different locations on each slide, and the results are presented for cell nuclei (B) and the cytoplasm (C). The cells were also harvested for an analysis of HMGB1 production by real-time PCR (D). Culture supernatants were analyzed by ELISA after 8 h (E) or 24 h (F). Data represent the mean ± SEM from three independent experiments. (*) Compared to unstimulated conditions, $*P < 0.05$, $**P < 0.01$, $\#\#P < 0.01$, $***P < 0.001$ by one-way ANOVA. (For interpretation of the references to colour in this figure legend, the reader is referred to the web version of this article.)

treatment of MM-1 cells during co-culture significantly reduced the expression of the occludin gene in HBMECs compared with HBMECs cultured alone (Fig. 3D). We also determined that ZO expression was downregulated under all co-culture conditions (Fig. 3E). Collectively, these results suggest that ZIKV-infected cells release HMGB1 and dysregulate the expression of tight junction markers, affecting the integrity of HBMECs.

### 3.4. CCR7 expression in MM-1 cells increases in response to ZIKV infection

Knowing that CCR7 expression tightly regulates monocytes transmigration through the BBB, we characterized the effects of increasing times of ZIKV (MOI of 0.5) exposure (2, 8, and 24 h) on CCR7 transcription in MM-1 cells. Results showed that CCR7 mRNA expression was significantly increased after 8 h compared with uninfected cells (Fig. 4A). In contrast, the expression of CCR2, which has also been implicated in monocyte chemotaxis, was decreased after 8 h (Fig. 4B). These results demonstrate that ZIKV-mediated changes in the expression of CCR7, TNF-α, IL-10, and IL1-β are time dependent (Fig. 4A, C–E). Experiments were repeated in the context of LPS-induced inflammation. Treatment of MM-1 cells with 0.1 μg/mL LPS in combination with ZIKV infection (MOI of 0.5) also significantly upregulated CCR7 and IL1-β transcription, whereas there was no change in the levels of TNF-α mRNA (Fig. 5A, C, E). Moreover, CCR2 expression was downregulated under all stimulatory conditions, and IL-10 expression was higher after LPS treatment combined with ZIKV infection compared to infection alone (Fig. 5A, B, D).

### 3.5. LPS activation facilitates the "Trojan Horse" migration of MM-1 cells through the BBB via CCR7 maintenance

We next evaluated whether increased production of CCR7 mRNA during ZIKV infection correlates with the migration of MM-1 cells. MM-1 cells were infected with ZIKV for 8 h before assaying their migration through polycarbonate filters after 4 h. The results of the chemotaxis assay showed that ZIKV infection enhances the migration of MM-1 cells in response to CCL19, the natural ligand of CCR7 (Fig. 6). In contrast, infection with ZIKV for 8 h had no effect on the migration of MM-1 cells in response to the natural ligand of CCR2, CCL2 (Fig. 6). This assay was performed to determine whether the migration of the cells is affected by the presence of an endothelial barrier.

Although the migration of ZIKV-infected MM-1 cells was demonstrated in response to CCL19 using polycarbonate filters, migration in response to CCL19 using the BBB model was observed only when the cells were also activated by LPS (Fig. 7). Collectively, our chemotaxis assay results show that the migration of MM-1 cells infected with ZIKV in the BBB transmigration model is dependent on the presence of inflammation.

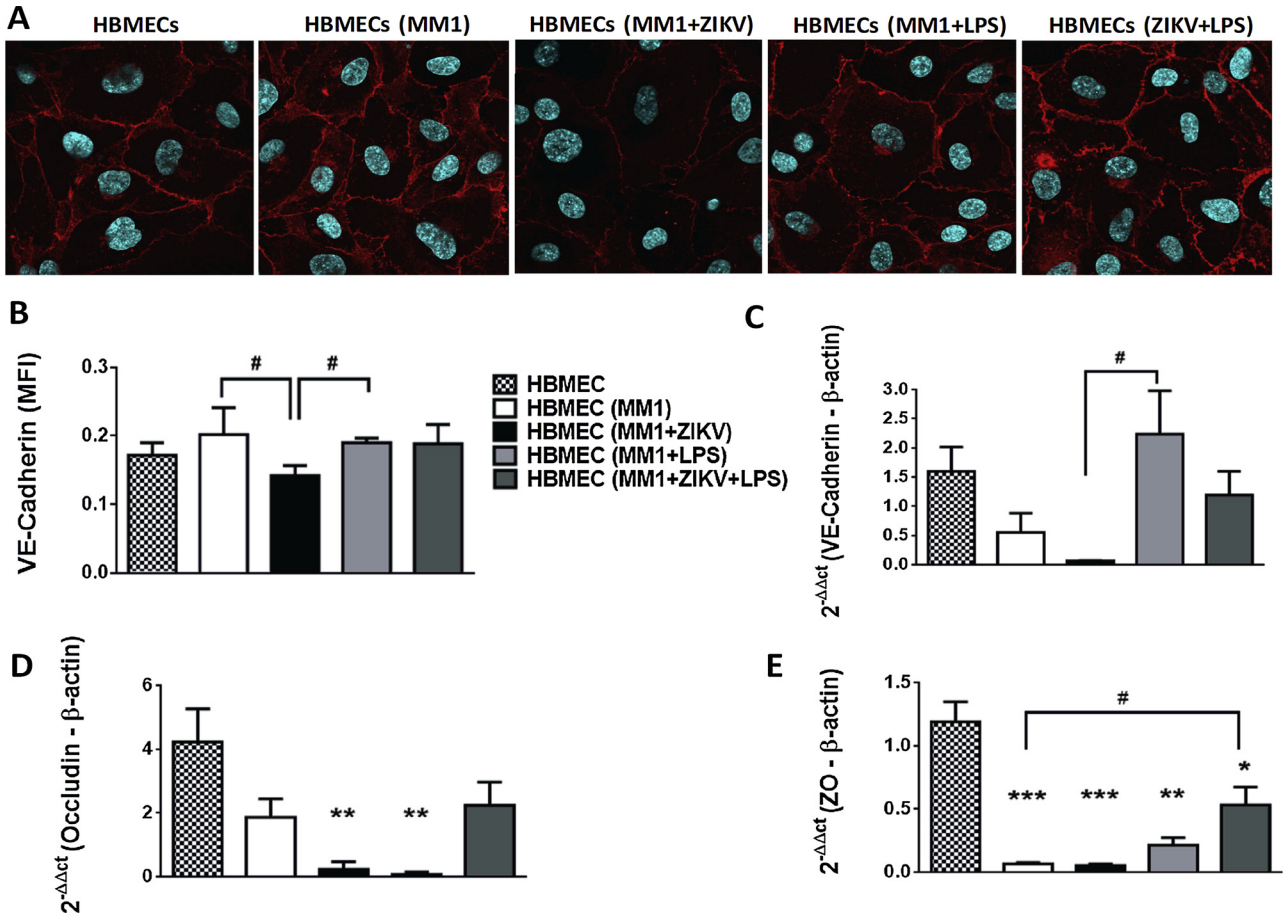


**Fig. 3.** ZIKV-infected MM-1 cells alter VE-cadherin protein and mRNA expression, and disrupt junctions between HBMECs. MM-1 cells were infected with ZIKV (MOI of 0.5), treated with 0.1 μg/mL LPS (TLR4), or infected and activated simultaneously for 8 h. HBMECs ($2 \times 10^5$/mL) were seeded into a glass-well cell culture chamber. Upon reaching confluence, HBMECs were cultured with MM-1 cells for 4 h. Cells were then fixed with 4% paraformaldehyde. Primary antibodies against VE-cadherin and NorthernLights 557-conjugated (red) secondary antibodies were used. DAPI (blue) was utilized for the visualization of the cell nucleus (40×) (A). MFI was measured in at least 10 different locations in each chamber (B). All cells were harvested and analyzed for the production of VE-cadherin (C), occludin (D), and ZO (E). Data represent the mean ± SEM from three independent experiments. (∗) Compared to HBMECs alone, *$P < 0.05$, **$P < 0.01$, ***$P < 0.001$, #$P < 0.05$ by one-way ANOVA. (For interpretation of the references to colour in this figure legend, the reader is referred to the web version of this article.)

### *3.6. ZIKV infection induces RAGE following contact between HBMECs and ZIKV-infected MM-1 cells*

HMGB1 is known to interact with high affinity with RAGE, which affects cell proliferation, growth, and migration (Taguchi et al., 2000; Palumbo et al., 2004; Vogel et al., 2016). Knowing that viral infections have been shown to modulate RAGE expression (van Zoelen et al., 2009; Nosaka et al., 2015; Zhu et al., 2016), we investigated whether LPS (0.1 μg/mL) stimulation in the presence or absence of ZIKV infection (MOI of 0.5) affected RAGE expression. To address this question, we treated and/or infected MM-1 cells and co-cultivated them with HBMECs. In immunofluorescence protein analyses, RAGE MFI was higher in HBMECs when ZIKV-infected MM-1 cells had been in contact with the endothelial cell layer for 4 h (Fig. 8A, C). Increased RAGE protein levels were observed when HBMECs were co-cultivated with MM-1 cells activated with LPS and infected with ZIKV. Expression of RAGE mRNA was also increased under these conditions (Fig. 8A, C, E). Increased RAGE protein levels were observed only in the cytoplasm of MM-1 cells infected with ZIKV (MOI of 0.5) (Fig. 8B, D). These results demonstrated that the presence of LPS during ZIKV infection of MM-1 cells affects RAGE protein levels and mRNA expression.

### *3.7. Blockade of RAGE reduces the migration of ZIKV-infected MM-1 cells through the BBB and controlled CCR7-induced migration*

FPS-ZM1 is a designed molecule that blocks ligands from binding to RAGE; it is non-toxic and readily crosses the BBB (Deane et al., 2012). We next addressed the potential capacity of FPS-ZM1 to inhibit MM-1 ZIKV "Trojan Horse" transmigration by controlling RAGE expression. FPS-ZM1 (1, 10, 100 nM) was added to cell cultures for 2 h prior to the transmigration assay, either directly to ZIKV-infected cells (Fig. 9, white bars) or HBMECs in culture (Fig. 9, black bars). We observed a substantial decrease in the migration of MM-1 ZIKV-infected cells and ZIKV-infected/LPS-stimulated cells when FPS-ZM1 was added to cultures (Fig. 9). Moreover, the highest dose of FPS-ZM1 examined (100 nM) was associated with greater inhibition of CCR7/CCL19 migration dependence in LPS-activated/ZIKV-infected cells (Fig. 9). Taken together, these results suggest that the extracellular release of HMGB1 during ZIKV infection is required for RAGE to upregulate CCR7 and increase the ability of monocytes to migrate through the BBB.

## 4. Discussion

Flaviviruses infect the human CNS and cause a variety of neurologic conditions, such as encephalitis, meningitis, meningoencephalitis, and paraplegia (Dick et al., 1952; Schuler-Faccini et al., 2016). Although all flaviviruses are known to cause neurologic sequelae in adults, only

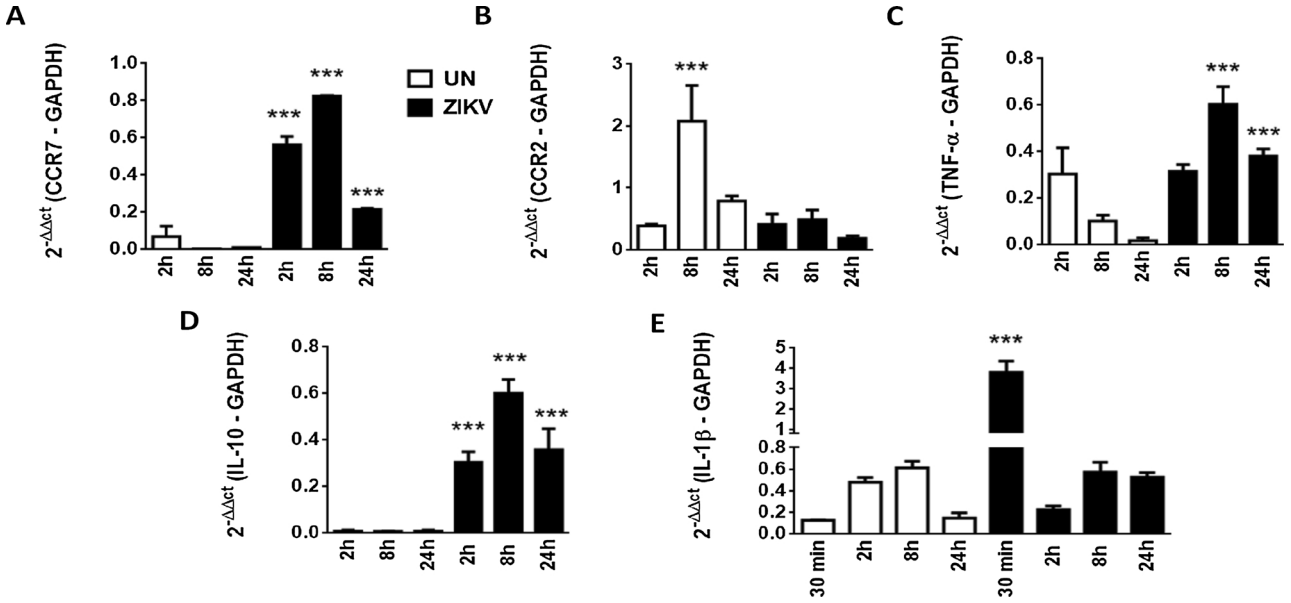


**Fig. 4.** ZIKV (ATCC VR1838) infection increases CCR7, TNF-α, IL-10, and IL-1β mRNA expression in MM-1 cells. MM-1 cells were infected with ZIKV at an MOI of 0.5, and the cells were harvested at 30 min, and at 2, 8, and 24-h postinfection and further analyzed for the production of CCR7 (A), CCR2 (B), TNF-α (C), IL-10 (D), and IL-1β (E) using real-time PCR. Unstimulated (UN) cells were used as the negative control and harvested at the same times as ZIKV-infected cells. Data represent the mean ± SEM from three independent experiments. ***$P < 0.001$ by one-way ANOVA, *Represents the difference between unstimulated samples at the same time point.

ZIKV has been shown to cause congenital neurologic disease in humans (Dick et al., 1952). Monocytes have been linked with the transmission and pathogenesis of ZIKV (Foo et al., 2017; Michlmayr et al., 2017; Kam et al., 2017). The migration of monocytes occurs during inflammation in the CNS. The dysregulation of migration during infection suggests these cells have effector functions that could result in a range of neurologic side effects. As such, determining how ZIKV-infected monocytes are recruited to the CNS as "Trojan Horse" cells is of critical importance. In this study, we developed for the first time an outline model of CCR7 and RAGE control during transmigration of ZIKV-infected monocytes through the BBB. We demonstrated that MM-1 cells are useful representatives of monocytes during ZIKV infection. Although we utilized a dose above the TCID50/mL determined in 4-day assays using Vero cells (data not shown), our results showed that a $10^{-2}$ dilution was not associated with an increase in apoptosis, perhaps because MM-1 cells are non-adherent and we used at a least a 24-h course of infection. Viral load and *Flavivirus* E protein were monitored during the assays in order to ensure that cell integrity was maintained during BBB transmigration.

Our group previously showed that TLR4 activation by LPS modulates CCR7 mRNA expression and increases monocyte transmigration through the BBB (Paradis et al., 2016a). Our results in the present study also showed that ZIKV infection increases CCR7 gene expression, with a peak after 8 h of exposure. The mRNA expression of other markers, such

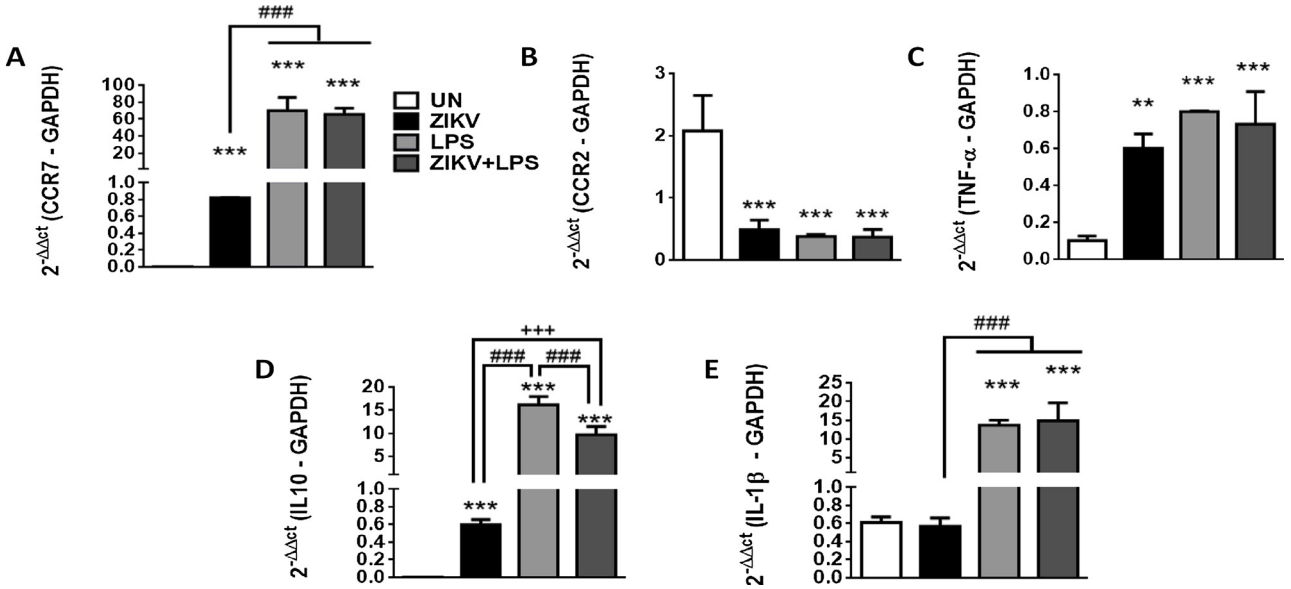


**Fig. 5.** TLR4 activation by LPS upregulates CCR7 and IL-1β mRNA expression in ZIKV-infected MM-1 cells. MM-1 cells were infected with ZIKV, activated with 0.1 μg/mL LPS, or infected and activated simultaneously. After 8 h, the cells were harvested to determine the production of CCR7 (A), CCR2 (B), TNF-α (C), IL-10 (D), and IL1-β (E) using real-time PCR. Data represent the mean ± SEM from three independent experiments. ∗Compared to the unstimulated condition. **$P < 0.01$, ***$P < 0.001$, ###$P < 0.001$, +++$P < 0.001$ by one-way ANOVA.

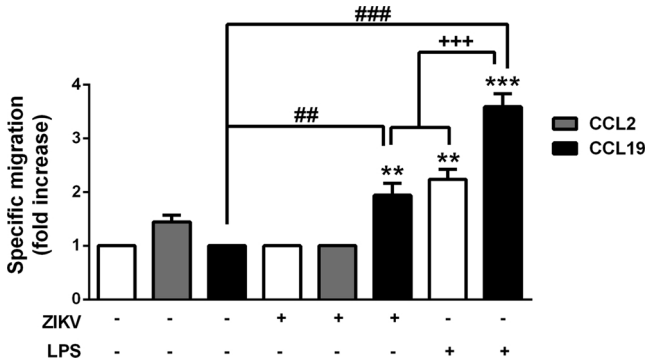


**Fig. 6.** ZIKV activation modulates CCR7 function in MM-1 cells. Chemotaxis of MM-1 cells infected with ZIKV (MOI of 0.5) or treated with 0.1 μg/mL LPS (TLR4) for 8 h was assessed in the presence of 300 ng/mL CCL19 (filled black bars), 30 ng/mL CCL2 (filled gray bars), or medium alone (white bars). The mean number of cells that spontaneously migrated (in response to medium alone) after 4 h was subtracted from the number of cells that migrated in response to CCL19 or CCL2. Data represent the mean ± SEM of five independent experiments. ∗Compared to unstimulated condition, $^{**}P < 0.01$, $^{***}P < 0.001$, $\#\#P < 0.01$, $\#\#\#P < 0.001$, $+++P < 0.001$ by one-way ANOVA.

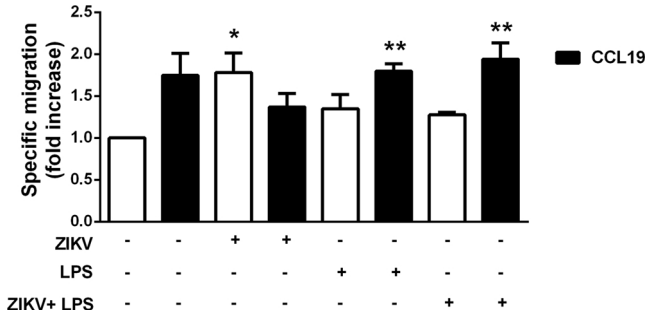


**Fig. 7.** LPS activation facilitates the migration of ZIKV-infected MM-1 cells through the BBB via CCR7 maintenance. Chemotaxis of MM-1 cells infected with ZIKV (MOI of 0.5), 0.1 μg/mL LPS (TLR4), or infected and activated simultaneously in response to 300 ng/mL CCL19 (filled black bars) or medium alone (white bars) was assessed at 8 h. The mean number of cells that spontaneously migrated (in response to medium alone) at 4 h was subtracted from the number of cells that migrated in response to CCL19. Data represent the mean ± SEM of five independent experiments. ∗Compared to unstimulated condition, $^{*}P < 0.05$, $^{**}P < 0.01$ by one-way ANOVA.

as TNF-α and IL-10, was also evaluated, with increased levels observed during the same time period. Increased mRNA expression of IL-1β was detected early, at 30 min after the initiation of infection. LPS is recognized as an inducer of neuroinflammation and neurotoxicity, and has been used to study neurological disorders (Abreu et al., 2018; Olajide et al., 2013; Gao et al., 2002; Hu et al., 2012; Kempuraj et al., 2017). Interestingly, and knowing that *Flavivirus* RNA may be detected by TLRs and that infection of ZIKV in neurospheres can upregulate the levels of TLR4, a receptor that mediates the innate immune response against other neurotropic flaviviruses (Szretter et al., 2009; Han et al., 2014), we evaluated whether TLR4 plays a role in the transmigration of ZIKV-infected monocytes. We found similar but higher levels of CCR7, IL-10, and IL-1β in cultured MM-1 cells in the presence of LPS. This proinflammatory milieu correlated with the increased HMGB1 levels secreted into the supernatant of MM-1 cell cultures after 8 h. Our results are consistent with those reported by other groups, indicating that HMGB1 induces monocytes to produce TNF-α and IL-1β (Yan et al., 1996; Andersson et al., 2000).

HMGB1 is a DAMP molecule that induces the disruption of the endothelial cell barrier, resulting in enhanced monocyte migration (Wolfson et al., 2011; Ong et al., 2012; Shirasuna et al., 2016). HMGB1 also acts as a sensor by binding to LPS, which increases TLR4 signaling and NF-κB activation (Youn et al., 2008, 2011). In the present study, we detected HMGB1 in the nuclei of ZIKV-infected cells in the presence of LPS after 8 h. This finding may be explained by the fact that ZIKV suppresses the activation of JAK-STAT signaling by inducing the degradation of JAK1. Indeed, the inhibition of JAK/STAT was previously shown to block LPS-induced HMGB1 translocation to the cytoplasm (Lu et al., 2014; Wu et al., 2017). Additionally, STAT1-deficient mice demonstrate high sensitivity to ZIKV infection, which is accompanied by increased lethality (Kamiyama et al., 2017). Moreover, acetylated HMGB1 accompanied by LPS activation redirects HMGB1 to the cytosol, leading to its secretion by lysosomes (Bonaldi et al., 2003). We believe that the rapid secretion of the HMGB1 protein by MM-1 cells, confirmed by our ELISA results, might also be related to the low turnover of HMGB1 mRNA during our analysis period.

Our results demonstrate that MM-1 cells infected with ZIKV migrate through polycarbonate filters in response to the CCR7 natural ligand CCL19, whereas specific migration in response to CCL19 in the BBB model occurred when ZIKV-infected MM-1 cells were treated in conjunction with LPS for 8 h (0.1 μg/mL). This can be explained in that our analysis showed that CCR7 mRNA levels were markedly increased in the presence of LPS during infection and the barrier limited the number of cells able to migrate. Moreover, CCL19 binds to human CCR7 with slightly higher affinity than CCL21 (Ott et al., 2006). In addition, CCL2-induced migration was not observed, perhaps because CCR2 mRNA expression was low 8 h after ZIKV infection or LPS activation of MM-1 cells. Results obtained by a separate group showed that ZIKV strain Nica 2–16 upregulates CCL2 gene expression in human monocytes without any corresponding changes in CCR2 mRNA expression (Michlmayr et al., 2017). We know that *in vitro* assays using virus-infected animals is both technically and ethically challenging; therefore, the functional utility of "Trojan Horse" cell migration through the BBB should be considered. Although we used an adult human endothelial cell culture system, we understand that this does not represent a fetal brain. The levels of CCL19 found during brain inflammation are difficult to predict, since they depend on the extent of damage that might occur during a neurotropic virus infection or other neurological inflammatory disease. We are seeking to develop new *in vivo* and *in vitro* BBB models to better understand the physiological relevance of CCL19 during the migration of ZIKV-infected monocytes in the presence of injured brains. Moreover, a possible relationship between ZIKV infection and neurological complications in adults has also been proposed during epidemics in Oceania and South America, especially during an observed increased incidence of Guillain-Barré syndrome in French Polynesia (Oehler et al., 2014; Ioos et al., 2014). Collectively, our results demonstrate that ZIKV infection and LPS activation of MM-1 cells affects monocyte migration in response to CCL19. However, we must note that further studies using freshly isolated monocytes and the development of a transmigration system using fetal brain endothelial cells are needed to confirm these results.

Flaviviruses have been shown to induce increased expression of various cell surface proteins, such as ICAM1, VCAM-1, and E-selectin, ligands that interact with leukocyte integrins to increase adhesion to the endothelial cells (King and Kesson, 2003; Roe et al., 2014). Other research has shown that HMGB1 protein released during DENV infection by infected PBMCs is capable of potentiating vascular permeability of umbilical cord vein endothelial cells (Ong et al., 2012). In the context of a congenital infection, HMGB1 facilitates the migration of monocytes by increasing the permissiveness of endothelial cells during pregnancy (Shirasuna et al., 2016). Increased production of HMGB1 favors the loss of endothelial junctions accompanied by the disorganization of actin fibers and dissociation of cadherins, which can be reversed by the use of siRNAs (Wolfson et al., 2011; Fraisiera et al., 2015). Cell migration via the BBB may also occur due to the secretion of HMGB1 during ZIKV infection. However, the exact mechanism by which ZIKV crosses BBB and causes neurologic complications is unknown (Miner and Diamond,

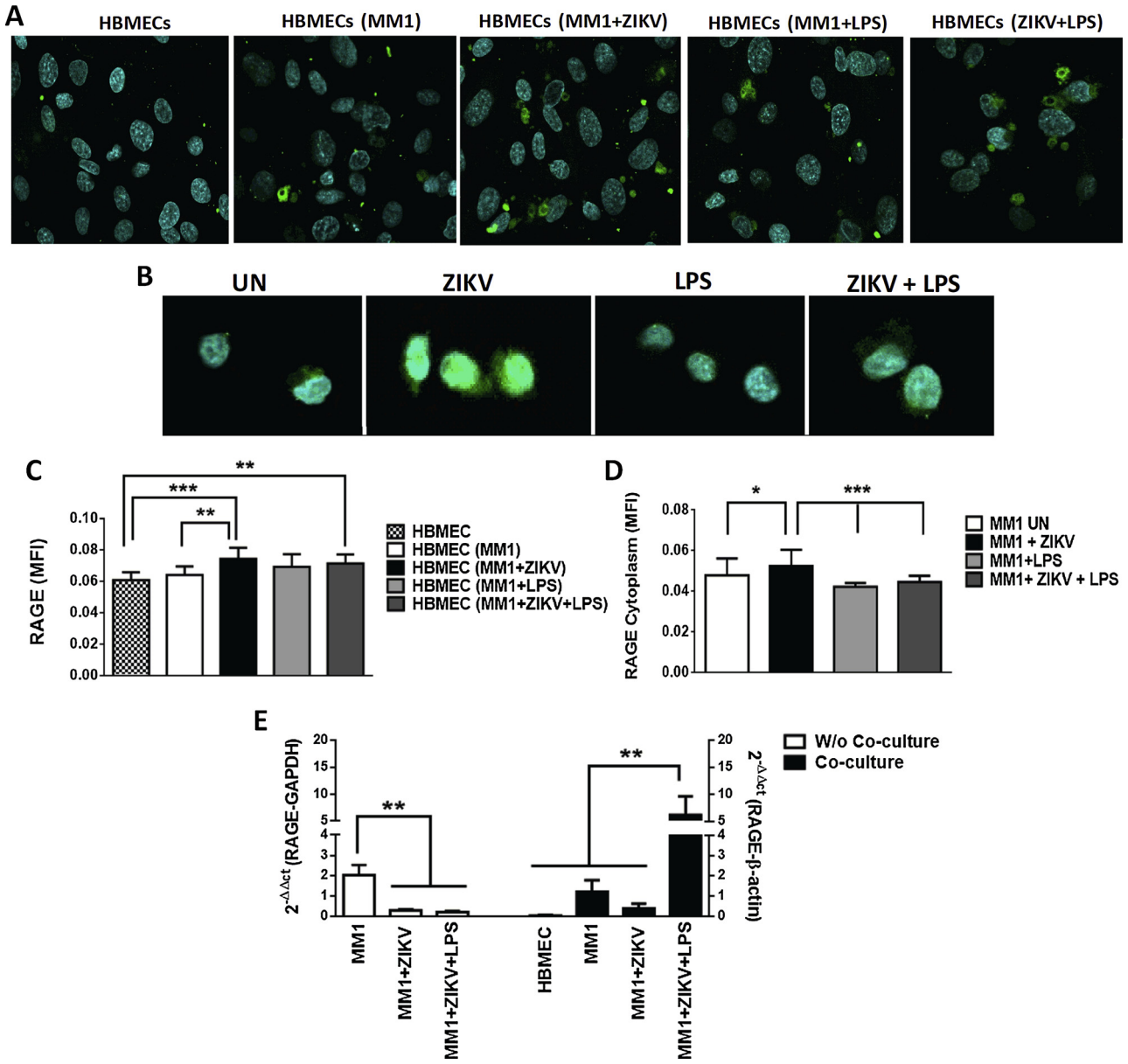


**Fig. 8.** RAGE protein was modulated by ZIKV infection or contact between HBMECs and infected cells. MM-1 cells were infected with ZIKV (MOI of 0.5) and treated or not with 0.1 μg/mL LPS for 8 h and co-cultured or not with HBMECs for 4 h. After LPS stimulation or an additional 4 h of co-culture, the cells were fixed with 4% paraformaldehyde. Primary antibodies against RAGE and NorthernLights NL493-conjugated (green) secondary antibodies were used. DAPI (blue) was utilized for the visualization of the cell nucleus (40×) (A, B). The MFI of the cells was measured in at least 10 different locations in each chamber or on each slide (C, D). All cells were harvested for an analysis of RAGE expression by real-time PCR (E). Data represent the mean ± SEM from three independent experiments. $^{*}P < 0.05$, $^{**}P < 0.01$, $^{***}P < 0.001$ by one-way ANOVA. (For interpretation of the references to colour in this figure legend, the reader is referred to the web version of this article.)

2016). Other groups have shown that ZIKV can infect, activate, and cross endothelial cells without barrier disruption (Papa et al., 2017). However, we observed that HMGB1 levels in the supernatant of MM-1 cell cultures was significantly increased 8 h after ZIKV infection. Our results strongly suggest that during co-culture, HMGB1 released by infected monocytes in the culture supernatant, together with other proinflammatory factors (e.g., TNF-α and IL-1β), induce the dysregulation of endothelial cell junction components such as VE-cadherin, occludin, and ZO. However, the differences in VE-cadherin, occludin, and ZO gene expression in HBMECs observed during ZIKV infection of MM-1 cells, with or without LPS, might be related to the gene regulatory activity of HMGB1 in MM-1 cells and the levels of HMGB1 secreted during the different treatments.

RAGE is a pattern-recognition receptor that plays a role in innate immune responses, and it is highly expressed in the embryonic CNS (Hori et al., 1995). In adult endothelial cells, monocytes, microglia, and neurons, RAGE is expressed at low levels (Brett et al., 1993). RAGE expression is upregulated upon interaction with various proinflammatory molecules, such as HMGB1 (Casula et al., 2011), nucleic acids (Sirois et al., 2013), and lysophosphatidic acid (Rai et al., 2012a,b). However, the results of our study suggest that HMGB1 secreted by ZIKV-infected MM-1 cells is associated with increased RAGE protein levels, as evidenced by the observed increase in RAGE MFI in the cytoplasm of infected cells. Moreover, ZIKV-infected MM-1 cells co-cultured with HBMECs also exhibited increased RAGE fluorescence in locations where cells had previously contacted HBMECs. In contrast, LPS-activated/ZIKV-infected MM-1 cells exhibited increased RAGE levels only when co-cultured with HBMECs. This observation can be

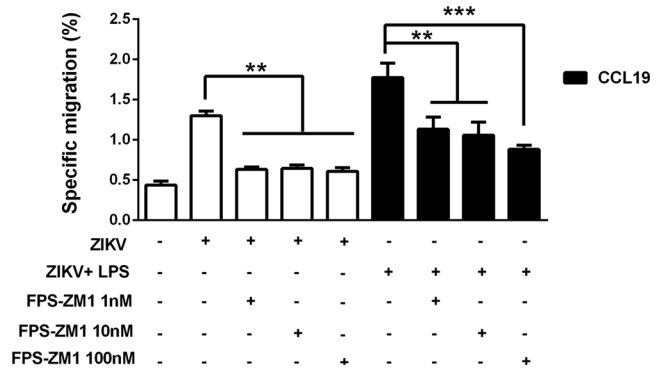


**Fig. 9.** FPS-ZM1 reduces the migration of ZIKV-infected MM-1 cells through the BBB and controls the dependence of TLR4-activated/ZIKV-infected cell migration on CCR7. Chemotaxis assays using 300 ng/mL CCL19 (black bars) or medium alone (white bars) were performed using MM-1 cells infected with ZIKV (MOI of 0.5) or TLR4-activated/ZIKV-infected MM-1 cells for 8 h. FPS-ZM1 (1, 10, 100 nM) was added for 2 h prior to the transmigration assay either directly to ZIKV-infected cells (white bars) or HBMECs in culture (black bars). The mean number of spontaneously migrated cells (migration in response to medium alone) was subtracted from the number of cells that migrated in response to CCL19. Data represent the mean ± SEM of three independent experiments. $^{**}P < 0.01$, $^{***}P < 0.001$ by one-way ANOVA.

explained by competition for binding sites between LPS and HMGB1 for binding to RAGE and TLR4. Finally, we demonstrated that addition of FPS-ZM1 (a RAGE inhibitor) prior to the transmigration assay either directly to ZIKV-infected cells or to HBMECs during culture results in a marked decrease in RAGE-dependent transmigration. Previous work showed that both the migration of monocytes and neuroinflammation could be inhibited by FPS-ZM1 treatment (Giri et al., 2000; Deane et al., 2012). Other studies have shown that HMGB1 mediates cytoskeletal reorganization; the blockade of HMGB1/RAGE by neutralizing antibodies prevents the upregulation of CCR7 and the migratory function of mature DCs (Dumitriu et al., 2007). Unfortunately, we did not investigate the cross-talk between RAGE and CCR7. MAPK members are well-known regulators of chemotaxis in DCs, and the CCR7/CCL19 signaling pathway induces a Gi-dependent activation of MAPK members ERK1/2, JNK, and p38 (Riol-Blanco et al., 2005). Blockade of RAGE has been shown to elicit direct effects on ERK1/2, JNK, and p38, impairing cellular migration (Liu et al., 2010). However, our results suggest that the concentration of FPS-ZM1 used to block RAGE might favor a reduction in CCR7/CCL19 migration by interfering with the MAPK signaling pathway. CCR7-dependent migration can also be directly inhibited by the CCR7-derived synthetic peptide TM4 (Kobayashi et al., 2017). HBMECs also might express other adhesion molecules or chemokines that are able to activate monocyte integrins. Our present study focused on the role of RAGE and CCR7 in leukocyte transmigration across the BBB during viral infection. This work is based on the function of RAGE/CCR7 as a monocyte migration factor during ZIKV infection. In this context, the migration rates of MM-1 cells could differ from those of normal human monocytes, and this possibility requires further investigation.

Monocytes contribute to the pathogenesis of ZIKV and bacterial infections, and neuroinflammatory consequences may occur as a result of monocyte accumulation in the brain, particularly due to the delivery of neurotropic viruses via a “Trojan Horse” mechanism. Understanding the molecular role of monocyte trafficking during ZIKV infections, in the presence or absence of bacterial factors, could facilitate the development of new therapeutic strategies to prevent the deleterious consequences of ZIKV neuroinfections.

## Author’s declaration

This manuscript contains original work, and the actual material has not been previously reported and/or is not under consideration for publication elsewhere.

The authors declare that there are no conflicts of interest (financial or commercial) with the submitted material.

## Declaration of Competing Interest

The authors declare that there are no conflicts of interest (financial or commercial) with the submitted material.

## Acknowledgments

This work was supported, in part, by the Fundação de Amparo a Pesquisa do Estado de São Paulo (2017/22539-0) and (2016/08061-7), Laboratory of Medical Research, Unit 56 of the Hospital das Clínicas-Faculty of Medicine of São Paulo. This study was also supported by The Natural Sciences and Engineering Research Council of Canada (Funding Reference Number RGPIN-2015-06306).

## References

Abreu, C.M., Gama, L., Krasemann, S., Chesnut, M., Odwin-Dacosta, S., Hogberg, H.T., Hartung, T., Pamies, D., 2018. Microglia increase inflammatory responses in iPSC-derived human BrainSpheres. Front. Microbiol. 9. https://doi.org/10.3389/fmicb.2018.02766.

Allonso, D., Belgrano, F.S., Calzada, N., Guzmán, M.G., Vázquez, S., Mohana-Borges, R., 2012. Elevated serum levels of high mobility group box 1 (HMGB1) protein in dengue-infected patients are associated with disease symptoms and secondary infection. J. Clin. Virol. 55 (3), 214–219.

Andersson, U., Wang, H., Palmblad, K., Aveberger, A.C., Bloom, O., Erlandsson-Harris, H., Janson, A., Kokkola, R., Zhang, M., Yang, H., Tracey, K.J., 2000. High mobility group 1 protein (HMG-1) stimulates proinflammatory cytokine synthesis in human monocytes. J. Exp. Med. 192 (4), 565–570.

Anzilotti, S., Giampà, C., Laurenti, D., Perrone, L., Bernardi, G., Melone, M.A., Fusco, F.R., 2012. Immunohistochemical localization of receptor for advanced glycation end (RAGE) products in the R6/2 mouse model of Huntington’s disease. Brain Res. Bull. 87 (2–3), 350–358.

Bamboat, Z.M., Balachandran, V.P., Ocuin, L.M., Obaid, H., Plitas, G., DeMatteo, R.P., 2010. Toll-like receptor 9 inhibition confers protection from liver ischemia-reperfusion injury. Hepatology 51, 621–632.

Bayer, A., Lennemann, N.J., Ouyang, Y., Bramley, J.C., Morosky, S., Marques Jr., E.T.D.A., Cherry, S., Sadovsky, Y., Coyne, C.B., 2016. Type III interferons produced by human placental trophoblasts confer protection against Zika virus infection. Cell Host Microbe 19 (5), 705–712.

Bonaldi, T., Talamo, F., Scaffidi, P., Ferrera, D., Porto, A., Bachi, A., Rubartelli, A., Agresti, A., Bianchi, M.E., 2003. Monocytic cells hyperacetylate chromatin protein HMGB1 to redirect it towards secretion. EMBO J. 22, 5551–5560.

Gaillard, C., Borde, C., Barnay-Verdier, S., Hocini, H., Marechal, V., Gozlan, J., 2011. Stepwise release of biologically active HMGB1 during HSV-2 infection. PLoS One 6, e16145.

Brenn, A., Grube, M., Peters, M., Fischer, A., Jedlitschky, G., Kroemer, H.K., Warzok, R.W., Vogelgesang, S., 2011. Beta-amyloid downregulates MDR1-P-glycoprotein (Abcb1) expression at the blood-brain barrier in mice. Int. J. Alzheimers Dis. 2011.

Brett, J., Schmidt, A.M., Du Yan, S., Zou, Y.S., Weidman, E., Pinsky, D., Nowygrod, R., Neeper, M., Przysiecki, C., Shaw, A., Migheli, A., 1993. Survey of the distribution of a newly characterized receptor for advanced glycation end products in tissues. Am. J. Pathol. 143 (6), 1699.

Casula, M., Iyer, A.M., Spliet, W.G.M., Anink, J.J., Steentjes, K., Sta, M., Troost, D., Aronica, E., 2011. Toll-like receptor signaling in amyotrophic lateral sclerosis spinal cord tissue. Neuroscience 179, 233–243.

Chu, J.J., Ng, L.M., 2003. The mechanism of cell death during West Nile virus infection is dependent on initial infectious dose. J. Gen. Virol. 84, 3305–3314.

Columba-Cabezas, S., Elena, B.S., Aloisi, A.F., 2003. Lymphoid chemokines CCL19 and CCL21 are expressed in the central nervous system during experimental autoimmune encephalomyelitis: implications for the maintenance of chronic neuroinflammation. Brain Pathol. 13 (1), 38–51.

Coté, S.C., Pasvanis, S., Bounou, S., Dumais, N., 2009. CCR7-specific migration to CCL19 and CCL21 is induced by $PGE_2$ stimulation in human monocytes: involvement of $EP_2$/$EP_4$ receptors activation. Mol. Immunol. 46, 2682–2693.

Deane, R., Singh, I., Sagare, A.P., Bell, R.D., Ross, N.T., LaRue, B., Love, R., Perry, S., Paquette, N., Deane, R.J., Thiyagarajan, M., 2012. A multimodal RAGE-specific inhibitor reduces amyloid β–mediated brain disorder in a mouse model of Alzheimer disease. J. Clin. Invest. 122 (4), 1377–1392.

Delorme-Axford, E., Sadovsky, Y., Coyne, C.B., 2014. The placenta as a barrier to viral infections. Annu. Rev. Virol. 1, 133–146.

Dick, G.W.A., Kitchen, S.F., Haddow, A.J., 1952. Zika virus (I). Isolations and serological specificity. Trans. R. Soc. Trop. Med. Hyg. 46 (5), 509–520.

Yan, S.D., Chen, X., Fu, J., Chen, M., Zhu, H., Roher, A., Slattery, T., Zhao, L., Nagashima, M., Morser, J., Migheli, A., 1996. RAGE and amyloid-β peptide neurotoxicity in

Alzheimer's disease. Nature 382 (6593), 685.
Dumitriu, I.E., Bianchi, M.E., Bacci, M., Manfredi, A.A., Rovere-Querini, P., 2007. The secretion of HMGB1 is required for the migration of maturing dendritic cells. J. Leukoc. Biol. 81 (1), 84–91.
Dumitriu, I.E., Baruah, P., Valentinis, B., Voll, R.E., Herrmann, M., Nawroth, P.P., Arnold, B., Bianchi, M.E., Manfredi, A.A., Rovere-Querini, P., 2005. Release of high mobility group box 1 by dendritic cells controls T cell activation via the receptor for advanced glycation end products. J. Immunol. 174, 7506–7515.
Foo, S.S., Chen, W., Chan, Y., Bowman, J.W., Chang, L.C., Choi, Y., Yoo, J.S., Ge, J., Cheng, G., Bonnin, A., Nielsen-Saines, K., 2017. Asian Zika virus strains target CD14+ blood monocytes and induce M2-skewed immunosuppression during pregnancy. Nat. Microbiol. 2 (11), 1558.
Fraisiera, C., Papab, A., Almerasa, L., 2015. High-mobility group box-1, promising serological biomarker for the distinction of human WNV disease severity. Virus Res. 195, 9–12.
Gao, H.M., Jiang, J., Wilson, B., Zhang, W., Hong, J.S., Liu, B., 2002. Microglial activation-mediated delayed and progressive degeneration of rat nigral dopaminergic neurons: relevance to Parkinson's disease. J. Neurochem. 81, 1285–1297. https://doi.org/10.1046/j.1471-4159.2002.00928.x.
Giri, R., Shen, Y., Stins, M., Du Yan, S., Schmidt, A.M., Stern, D., Kim, K.S., Zlokovic, B., Kalra, V.K., 2000. β-Amyloid-induced migration of monocytes across human brain endothelial cells involves RAGE and PECAM-1. Am. J. Physiol.-Cell Physiol. 279 (6), C1772–C1781.
Han, Y.W., et al., 2014. Distinct dictation of Japanese encephalitis virus-induced neuroinflammation and lethality via triggering TLR3 and TLR4 signal pathways. PLoS Pathog. 10, e1004319.
Hori, O., Brett, J., Slattery, T., Cao, R., Zhang, J., Chen, J.X., Nagashima, M., Lundh, E.R., Vijay, S., Nitecki, D., Morser, J., 1995. The receptor for advanced glycation end products (RAGE) is a cellular binding site for amphoterin mediation of neurite outgrowth and co-expression of rage and amphoterin in the developing nervous system. J. Biol. Chem. 270 (43), 25752–25761.
Hu, X., Zhou, H., Zhang, D., Yang, S., Qian, L., Wu, H.M., et al., 2012. Clozapine protects dopaminergic neurons from inflammation-induced damage by inhibiting microglial overactivation. J. Neuroimmune Pharmacol. 7, 187–201. https://doi.org/10.1007/s11481-011-9309-0.
Ioos, S., Mallet, H.P., Leparc Goffart, I., Gauthier, V., Cardoso, T., Herida, M., 2014. Current Zika virus epidemiology and recent epidemics. Med. Mal. Infect. 44 (7), 302e7.
Kawano, Y., Ito, Y., Torii, Y., Ohta, R., Imai, M., Hara, S., et al., 2011. Increased levels of cytokine and high-mobility group box 1 are associated with the development of severe pneumonia, but not acute encephalopathy, in 2009 H1N1 influenza-infected children. Cytokine 56, 180–187.
Kam, Y.W., Leite, J.A., Lum, F.M., Tan, J.J., Lee, B., Judice, C.C., Teixeira, D.A.D.T., Andreata-Santos, R., Vinolo, M.A., Angerami, R., Resende, M.R., 2017. Specific biomarkers associated with neurological complications and congenital central nervous system abnormalities from Zika virus–infected patients in Brazil. J. Infect. Dis. 216 (2), 172–181.
Kamiyama, N., Soma, R., Hidano, S., Watanabe, K., Umekita, H., Fukuda, C., Sachi, N., 2017. Ribavirin inhibits Zika virus (ZIKV) replication in vitro and suppresses viremia in ZIKV-infected STAT1-deficient mice. Antiviral Res. 146, 1–11.
Kempuraj, D., Thangavel, R., Selvakumar, G.P., Zaheer, S., Ahmed, M.E., Raikwar, S.P., et al., 2017. Brain and peripheral atypical inflammatory mediators potentiate neuroinflammation and neurodegeneration. Front. Cell. Neurosci. 11, 216. https://doi.org/10.3389/fncel.2017.00216.
King, N.J., Kesson, A.M., 2003. Interaction of flaviviruses with cells of the vertebrate host and decoy of the immune response. Immunol. Cell Biol. 81 (3), 207–216.
Kobayashi, D., Endo, M., Ochi, H., Hojo, H., Miyasaka, M., Hayasaka, H., 2017. Regulation of CCR7-dependent cell migration through CCR7 homodimer formation. Sci. Rep. 7 (1), 8536.
Krumbholz, M., Theil, D., Steinmeyer, F., Cepok, S., Hemmer, B., Hofbauer, M., Farina, C., Derfuss, T., Junker, A., Arzberger, T., Sinicina, I., 2007. CCL19 is constitutively expressed in the CNS, up-regulated in neuroinflammation, active and also inactive multiple sclerosis lesions. J. Neuroimmunol. 190 (1–2), 72–79.
Liu, S., DeLalio, L.J., Isakson, B.E., Wang, T.T., 2016. AXL-mediated productive infection of human endothelial cells by Zika virus. Circ. Res. 119 (11), 1183–1189.
Liu, Y., Liang, C., Liu, X., Liao, B., Pan, X., Ren, Y., Wu, Z., 2010. AGEs increased migration and inflammatory responses of adventitial fibroblasts via RAGE, MAPK and NF-κB pathways. Atherosclerosis 208 (1), 34–42.
Lotze, M.T., Tracey, K.J., 2005. High-mobility group box 1 protein (HMGB1): nuclear weapon in the immune arsenal. Nat. Rev. Immunol. 5, 331–342.
Ludlow, M., KortekaasS, J., Herden, C., Hoffmann, B., Tappe, D., Trebest, C., et al., 2016. Neurotropic virus infection as the cause of immediate and delayed neuropathology. Acta Neuropathol. 5131, 159–185. https://doi.org/10.1007/s00401-015-1511-3.
Lu, B., Antoine, D.J., Kwan, K., Lundbäck, P., Wähämaa, H., Schierbeck, H., Erlandsson-Harris, H., 2014. JAK/STAT1 signaling promotes HMGB1 hyperacetylation and nuclear translocation. Proc. Natl. Acad. Sci. U. S. A. 111 (8), 3068–3073.
McGavern, D.B., Kang, S.S., 2011. Illuminating viral infections in the nervous system. Nat. Rev. Immunol. 11, 318–329.
Michlmayr, D., Andrade, P., Gonzalez, K., Balmaseda, A., Harris, E., 2017. CD14+ CD16+ monocytes are the main target of Zika virus infection in peripheral blood mononuclear cells in a paediatric study in Nicaragua. Nat. Microbiol. 2 (11), 1462.
Miner, J.J., Diamond, M.S., 2016. Mechanisms of restriction of viral neuroinvasion at the blood–brain barrier. Curr. Opin. Immunol. 38, 18–23.
Neal, J.W., 2014. Flavivirus are neurotropic, but do they invade the CNS? J. Infect. 69, 2013–2214. https://doi.org/10.1016/j.jinf.2014.05.010.
Nosaka, N., Yashiro, M., Yamada, M., Fujii, Y., Tsukahara, H., Liu, K., Morishima, T., 2015. Anti-high mobility group box-1 monoclonal antibody treatment provides protection against influenza A virus (H1N1)-induced pneumonia in mice. Crit. Care 19 (1), 249.
Nowak, P., Barqasho, B., Sonnerborg, A., 2007. Elevated plasma levels of high mobility group box protein 1 in patients with HIV-1 infection. AIDS 21, 869–871.
Oehler, E., Watrin, L., Larre, P., Leparc-Goffart, I., Lastere, S., Valour, F., et al., 2014. Zika virus infection complicated by Guillain-Barre syndrome e case report, French Polynesia, 2013. Euro Surveill. 19 (December (9)).
Olajide, O.A., Bhatia, H.S., de Oliveira, A.C., Wright, C.W., Fiebich, B.L., 2013. Inhibition of neuroinflammation in LPS-activated microglia by cryptolepine. Evid. Based Complement. Altern. Med. 2013, 459723. https://doi.org/10.1155/2013/459723.
Ong, S.P., Lee, L.M., Leong, Y.F.I., Ng, M.L., Chu, J.J.H., 2012. Dengue virus infection mediates HMGB1 release from monocytes involving PCAF acetylase complex and induces vascular leakage in endothelial cells. PLoS One 7 (7), e41932.
Ott, T.R., Lio, F.M., Olshefski, D., Liu, X.J., Ling, N., Struthers, R.S., 2006. The N-terminal domain of CCL21 reconstitutes high affinity binding, G protein activation, and chemotactic activity, to the C-terminal domain of CCL19. Biochem. Biophys. Res. Commun. 348 (3), 1089–1093.
Palumbo, R., Sampaolesi, M., De Marchis, F., Tonlorenzi, R., Colombetti, S., Mondino, A., Cossu, G., Bianchi, M.E., 2004. Extracellular HMGB1, a signal of tissue damage, induces mesoangioblast migration and proliferation. J. Cell Biol. 164 (3), 441–449.
Papa, M.P., Meuren, L.M., Coelho, S.V., Lucas, C.G., Mustafá, Y.M., Lemos Matassoli, F., Silveira, P.P., Frost, P.S., Pezzuto, P., Ribeiro, M.R., Tanuri, A., 2017. Zika virus infects, activates, and crosses brain microvascular endothelial cells, without barrier disruption. Front. Microbiol. 8, 2557.
Paradis, A., Bernier, S., Dumais, N., 2016a. TLR4 induces CCR7-dependent monocytes transmigration through the blood–brain barrier. J. Neuroimmunol. 295, 12–17.
Paradis, A., Leblanc, D., Dumais, N., 2016b. Optimization of an in vitro human blood–-brain barrier model: application to blood monocyte transmigration assays. MethodsX 3, 25–34.
Park, J.S., Gamboni-Robertson, F., He, Q., Svetkauskaite, D., Kim, J.Y., Strassheim, D., et al., 2006. High mobility group box 1 protein interacts with multiple Toll-like receptors. Am. J. Physiol. Cell Physiol. 290 (3), C917–C924.
Park, J.S., Svetkauskaite, D., He, Q., Kim, J.Y., Strassheim, D., Ishizaka, A., Abraham, E., 2004. Involvement of toll-like receptors 2 and 4 in cellular activation by high mobility group box 1 protein. J. Biol. Chem. 279, 7370–7377.
Rai, V., Maldonado, A.Y., Burz, D.S., Reverdatto, S., Schmidt, A.M., Shekhtman, A., 2012a. Signal transduction in Receptor for Advanced Glycation End Products (RAGE) solution structure of C-terminal RAGE (ctRAGE) and its binding to mDial. J. Biol. Chem. 287 (7), 5133–5144.
Rai, V., Touré, F., Chitayat, S., Pei, R., Song, F., Li, Q., Zhang, J., Rosario, R., Ramasamy, R., Chazin, W.J., Schmidt, A.M., 2012b. Lysophosphatidic acid targets vascular and oncogenic pathways via RAGE signaling. J. Exp. Med. 209 (13), 2339–2350.
Reed, L.J., Muench, H., 1938. A simple method of estimating fifty per cent endpoints. Am. J. Epidemiol. 27 (3), 493–497.
Riol-Blanco, L., Sánchez-Sánchez, N., Torres, A., Tejedor, A., Narumiya, S., Corbí, A.L., Rodríguez-Fernández, J.L., 2005. The chemokine receptor CCR7 activates in dendritic cells two signaling modules that independently regulate chemotaxis and migratory speed. J. Immunol. 174 (7), 4070–4080.
Roe, K., Orillo, B., Verma, S., 2014. West Nile virus-induced cell adhesion molecules on human brain microvascular endothelial cells regulate leukocyte adhesion and modulate permeability of the in vitro blood-brain barrier model. PLoS One 9 (7), e102598.
Saeki, H., Moore, A.M., Brown, M.J., Hwang, S.T., 1999. Cutting edge: secondary lymphoid-tissue chemokine (SLC) and CC chemokine receptor 7 (CCR7) participate in the emigration pathway of mature dendritic cells from the skin to regional lymph nodes. J. Immunol. 162, 2472–2475.
Schmidt, A.M., Du Yan, S., Yan, S.F., Stern, D.M., 2001. The multiligand receptor RAGE as a progression factor amplifying immune and inflammatory responses. J. Clin. Invest. 108 (7), 949–955.
Schuler-Faccini, L., Ribeiro, E.M., Feitosa, I.M., Horovitz, D.D., Cavalcanti, D.P., Pessoa, A., et al., 2016. Possible association between Zika virus infection and microcephaly e Brazil, 2015. MMWR Morb. Mortal. Wkly. Rep. 65 (3), 59–62.
Shirasuna, K., Seno, K., Ohtsu, A., Shiratsuki, S., Ohkuchi, A., Suzuki, H., Matsubara, S., Nagayama, S., Iwata, H., Kuwayama, T., 2016. AGE s and HMGB 1 increase inflammatory cytokine production from human placental cells, resulting in an enhancement of monocyte migration. Am. J. Reprod. Immunol. 75 (5), 557–568.
Sirois, C.M., Jin, T., Miller, A.L., Bertheloot, D., Nakamura, H., Horvath, G.L., Mian, A., Jiang, J., Schrum, J., Bossaller, L., Pelka, K., 2013. RAGE is a nucleic acid receptor that promotes inflammatory responses to DNA. J. Exp. Med. 210 (11), 2447–2463.
Steube, K.G., teepe, D.D., Meyer, C., et al., 1997. A model system in hematology and immunology: the human monocytic cell line MM-1. Leuk. Res. 21, 327–335.
Stros, M., 2010. HMGB proteins: interactions with DNA and chromatin. Biochim. Biophys. Acta 1799, 101–113.
Szretter, K.J., et al., 2009. The immune adaptor molecule SARM modulates tumor necrosis factor alpha production and microglia activation in the brainstem and restricts West Nile Virus pathogenesis. J. Virol. 83, 9329–9338.
Tabata, T., Petitt, M., Puerta-Guardo, H., Michlmayr, D., Wang, C., Fang-Hoover, J., Harris, E., Pereira, L., 2016. Zika virus targets different primary human placental cells, suggesting two routes for vertical transmission. Cell Host Microbe 20 (2), 155–166.
Taguchi, A., Blood, D.C., Del Toro, G., Canet, A., Lee, D.C., Qu, W., Tanji, N., Lu, Y., Lalla, E., Fu, C., Hofmann, M.A., 2000. Blockade of RAGE–amphoterin signalling suppresses tumour growth and metastases. Nature 405 (6784), 354.
Teismann, P., 2012. COX-2 in the neurodegenerative process of Parkinson's disease. Biofactors 38 (6), 395–397.

Vande Walle, L., Kanneganti, T.D., Lamkanfi, M., 2011. HMGB1 release by inflammasomes. Virulence 2, 162–165.
van Zoelen, M.A., van der Sluijs, K.F., Achouiti, A., Florquin, S., Braun-Pater, J.M., Yang, H., van der Poll, T., 2009. Receptor for advanced glycation end products is detrimental during influenza A virus pneumonia. Virology 391 (2), 265–273.
Vogel, S., Rath, D., Borst, O., Mack, A., Loughran, P., Lotze, M.T., Neal, M.D., Billiar, T.R., Gawaz, M., 2016. Platelet-derived high-mobility group box 1 promotes recruitment and suppresses apoptosis of monocytes. Biochem. Biophys. Res. Commun. 478, 143–148.
Warnock, R.A., Campbell, J.J., Dorf, M.E., Matsuzawa, A., McEvoy, L.M., Butcher, E.C., 2000. The role of chemokines in the microenvironmental control of T versus B cell arrest in Peyer's patch high endothelial venules. J. Exp. Med. 191, 77–88.
Weksler, B., Romero, I.A., Couraud, P.O., 2013. The hCMEC/D3 cell line as a model of the human blood brain barrier. Fluids Barriers CNS 10 (1), 16.
West, K.L., Castellini, M.A., Duncan, M.K., Bustin, M., 2004. Chromosomal proteins HMGN3a and HMGN3b regulate the expression of glycine transporter 1. Mol. Cell. Biol. 24, 3747–3756.
Wolfson, R.K., Chiang, E.T., Garcia, J.G., 2011. HMGB1 induces human lung endothelial cell cytoskeletal rearrangement and barrier disruption. Microvasc. Res. 81 (2), 189–197.
Wu, Y., Liu, Q., Zhou, J., Xie, W., Chen, C., Wang, Z., Cui, J., 2017. Zika virus evades interferon-mediated antiviral response through the co-operation of multiple nonstructural proteins in vitro. Cell Discov. 3, 17006.
Youn, J.H., Kwak, M.S., Wu, J., Kim, E.S., Ji, Y., Min, H.J., Yoo, J.H., Choi, J.E., Cho, H.S., Shin, J.S., 2011. Identification of lipopolysaccharide-binding peptide regions within HMGB1 and their effects on subclinical endotoxemia in a mouse model. Eur. J. Immunol. 41 (9), 2753–2762.
Youn, J.H., Oh, Y.J., Kim, E.S., Choi, J.E., Shin, J.S., 2008. High mobility group box 1 protein binding to lipopolysaccharide facilitates transfer of lipopolysaccharide to CD14 and enhances lipopolysaccharide-mediated TNF-α production in human monocytes. J. Immunol. 180 (7), 5067–5074.
Yu, M., Wang, H., Ding, A., Golenbock, D.T., Latz, E., Czura, C.J., Fenton, M.J., Tracey, K.J., Yang, H., 2006. HMGB1 signals through toll-like receptor (TLR) 4 and TLR2. Shock 26, 174–179.
Zeh, H.J., Lotze, M.T., 2005. Addicted to death: invasive cancer and the immune response to unscheduled cell death. J. Immunother. 28, 1–9.
Zhu, X., Sun, L., Wang, Y., 2016. High mobility group box 1 (HMGB1) is upregulated by the Epstein-Barr virus infection and promotes the proliferation of human nasopharyngeal carcinoma cells. Acta Otolaryngol. 136 (1), 87–94.